Chapter 2

Hydroxyapatite Production by an Intensification Process

Benedetta de Caprariis, Angelo Chianese, Marco Stoller and Nicola Verdone

Additional information is available at the end of the chapter

http://dx.doi.org/10.5772/intechopen.71775

Abstract

Hydroxyapatite (HAP) is a worthwhile compound for its biomedical applications. Nanoparticles (NPs) and nanostructured HAP scaffolds promote and intensify the interaction between artificial material and natural bone due to their high surface/volume ratio. In this chapter, first, the technique for the production of HPA nanoparticles smaller than 100 nm is addressed. It consists of the use of a rotating disk reactor to optimize the reaction-precipitation process. The centrifugal force dispersed into the liquid layer over the disk surface enables the attainment of micromixing conditions between the reagents and maximizes the reaction rate as a consequence. The reaction between calcium chloride and ammonium phosphate in the presence of ammonium hydroxide was adopted. NPs minimum size, equal to 78 μm, was obtained using a rotational velocity of 147 rad/s and feeding points of reagents 3 cm from the disk center. A computational fluid dynamics (CFD) model of the liquid layer was specifically developed for the interpretation of the obtained experimental results on the production of pure HAP. In the second part of the chapter, the feasibility of producing Mg^{2+} doped hydroxyapatite (Mg-HAP) by adding $MgCl_2$ and using the same technique is reported. Satisfactory results were obtained: nanoparticles were between 50 and 70 μm in size and Mg^{2+}/Ca^{2+} molar ratio was equal to 0.06, according to the composition target.

Keywords: hydroxyapatite, precipitation, spinning disk, micromixing, Mg-doped hydroxyapatite

1. Introduction

In recent years, several chemistry-based processing routes have been reported for preparing hydroxyapatite (HAP) powders. Nanoparticles with several morphologies have been synthesized by means of solid-state reaction, emulsion techniques, sol-gel and hydrothermal method [1];

however, the wet chemical precipitation method was proven to be one of the easiest ways for preparing HAP powders.

Wet chemical precipitation consists of a chemical reaction followed by the precipitation of the reaction product, which is a very sparingly solute. The overall process can be distinguished in several stages: the mixing among the reagents in liquid phase or gas-liquid phase, the reaction, the nucleation of solid particles as soon as the supersaturation has overcome the metastable limit, the growth and the aggregation of the solid particles. In order to produce solid nanoparticles, it is necessary to maximize nucleation rate and to minimize both growth and aggregation rate. In this respect, the key factor is the intensification of the mixing process. In fact, if the local mixing among the reagent streams, called micromixing, is very effective, the reagents locally attain the maximum concentration. As a consequence, the reaction rate takes place at the maximum rate, the maximum concentration of the required product, that is, its maximum supersaturation, is achieved and the nucleation rate is optimized.

According to the attained supersaturation, homogeneous or heterogeneous nucleation takes place. If the micromixing conditions are intense enough, the micromixing time is smaller than 1 ms and homogeneous nucleation becomes dominant with respect to heterogeneous one. In general, when the needed average crystal size is around one micron or smaller with tight crystal size distribution, homogeneous nucleation is preferred to heterogeneous nucleation. The major objective in this matter is, thus, to develop a precipitation reactor, which intensifies the mixing between the reagents much more than in a stirred reactor, in order to produce nanoparticles in a very narrow size range. For this purpose, microreactors, so-called T-mixer reactor and rotating disk reactor are adopted. All these reactors may assure conditions of micromixing, which usually induces homogeneous nucleation. More recently, the use of tubular microreactors have been proposed. Such apparatuses are characterized by very fast heat and mass transfer and a very small residence time of reagents fed to microstructured devices where the reactions are performed at very controlled conditions [2]. However, the application of this technique at the industrial scale seems to be hard to be proven. The T-mixer is often adopted as premixing device for precipitation-stirred reactors, but cannot represent a practical solution as a reactor stands alone, in particular for its needed high-dispersed energy. The rotating disk reactor requires lower energy amount with respect to the two above-mentioned reactors, may work in continuous mode and is of relatively simple scale-up. The present chapter is focused on the production process of nanoparticles of HAP, not-doped or Mg-doped, by using a spinning disk reactor (SDR).

The first attempt to use the SDR for a precipitation process was afforded by Cafiero et al. [3] by performing the wet precipitation of $BaSO_4$ over a disk rotating between 200 and 1000 rpm. In a subsequent paper, the same authors [4] calculated that at the highest rotational speed a micromixing time between the reagents smaller than 1 ms occurred and particles of barium sulfate around 0.5 μm in size were obtained. Moreover, a comparison between the T-mixer and the SDR performances, leading to the same micromixing, was made and it was shown that T-mixer is much energy consuming with respect to SDR.

Some other works reported the chance to use SDR to produce nanoparticles: Trippa et al. [5] studied the production of calcium carbonate particles from dissolved CO_2; Raston et al. [6]

showed the feasibility of producing b-carotene nanoparticles; Loh et al. [7] showed the potentiality of the spinning disk technology for large manufacture of chitosan nanoparticles; and finally Dabir et al. [8] present an experimental method for large-scale production of silver chloride nanoparticles using SDR.

In all these works, the importance of hydrodynamics of the liquid over the disk surface was emphasized. The prediction of the hydrodynamics over the SDR has been studied by many authors. The hydrodynamic simulation models were often evaluated with respect to the experimental values reported by Burns et al. [9], concerning the measurements of the liquid film thickness over a rotating disk. In the same paper, there was a comparison between the Pigford model and the Nusselt theory and it was shown that this latter cannot satisfactorily predict the liquid profiles over the disk when the inertial forces are higher than the viscous one, that is, for low values of the Ekman number. More recently, Bhatelia et al. [10] studied the prediction of the liquid layer over the rotating disk by a CFD model and they obtained results in good agreement with those reported by Burns. de Caprariis et al. [11] developed a CFD simulation model to predict the hydrodynamics of the reagent solutions over an SDR used for the production of hydroxyapatite. It was clearly shown both the patterns of the reagent streams fed over the disk and the progressively decrease of the reagents concentrations. The first work dealing with the production of nanoparticles in a two-phase solid liquid was that one of Plasari et al. [12]. Nucleation and growth were considered, whereas aggregation of particles was neglected. Some deviations between experimental and simulated values were obtained. More recently, de Caprariis et al. [13] tried to predict the crystallite of HPA produced over the spinning disk by inserting the particle balance equation in the CFD model previously developed by the same authors. Definitely, nowadays much work has to be done on the prediction of nanoparticles produced by means of an SDR.

In this chapter, the effects of several operating parameters (reagent flow rate, rotational speed and feed point location) on the size of pure HAP and Mg-HAP nanoparticles have been investigated. The nanoparticles size minimization for not-doped HAP, and for Mg-doped HAP at a fixed molar ratio Mg^{2+}/Ca^{2+} equal to 0.06, was pursued. The main aim has been to show the feasibility of producing nanoscale HAP nanoparticles by wet chemical synthesis in an SDR, by operating in continuous mode.

2. Description of the SDR system for the production of pure HAP and mg-HAP nanoparticles

Spinning disk reactor (SDR) appears to be a versatile and efficient equipment for the production of nanoparticles by wet chemical synthesis. As soon as chemical precipitation takes place under intensified micromixing conditions, a two-step nucleation-aggregation process mainly determines the size distribution of the produced nanoparticles. In these conditions, almost all the generated supersaturation is quickly consumed by nucleation, and only a small amount of the residual local supersaturation is available for growth and aggregation. First of all, it is interesting to point out the effect of the mixing intensification on the two main phenomena of

nucleation and aggregation. Hounslow and Mumtaz [14] have described the two-step process of aggregation: a shear stress orthokinetic collision between two particles and a subsequent cementation of these at their contact point due to internal diffusion of solute ions. In this process, fluid shear appears on the one hand to be in favor of aggregation by increasing the number and intensity of the particle collisions and on the other hand in disagreement, since it reduces the effect of the collisions due to reduced time for bridge formation and its disruptive action on the agglomerated particles. These considerations were derived from experimental runs on the aggregation of nanoparticles of calcium oxalate in a Poiseuille flow crystallizer. In this case, aggregation was reduced by intensified operating conditions, leading mainly to the disruptive action of the fluid shear stress. As a consequence, it appears that the mixing process intensification, enhancing nucleation and reducing aggregation process, leads to the production of smaller nanoparticles in size.

Some works emphasized the great importance of hydrodynamics on the produced particles size, taking into account the feeding points of the reagents over the disk surface. The paper of Parisi et al. [15] on the production of HAP particles pointed out the importance of the feed stream injection points over the disk to achieve specific particle size distributions and yields. Moreover, Stoller et al. [16] showed that the location of the injection points is very important with respect to the aggregation rate and the scaling formation over the reactor surface. In this chapter, the importance of the feed flow rate on the particle agglomeration was also observed, and in fact the density of the produced nanoparticles over the disk surface increases the aggregation rate.

Summarizing, the performances of a given SDR appear to be a function of the disk rotational speed, feed flow rate(s) and location of the injection points. The experimental device used in this work is schematized in **Figure 1**. It consists of a cylindrical case with an inner disk of 8.5 cm in diameter, made by PVC.

Rotational velocity of the disk could be increased up to 147 rad/s, corresponding to 1500 rpm. The reagent solutions were fed over the disk at a distance of 5 mm from the disk surface through tubes, 1 mm in diameter. The position of the reagent injection points over the disk

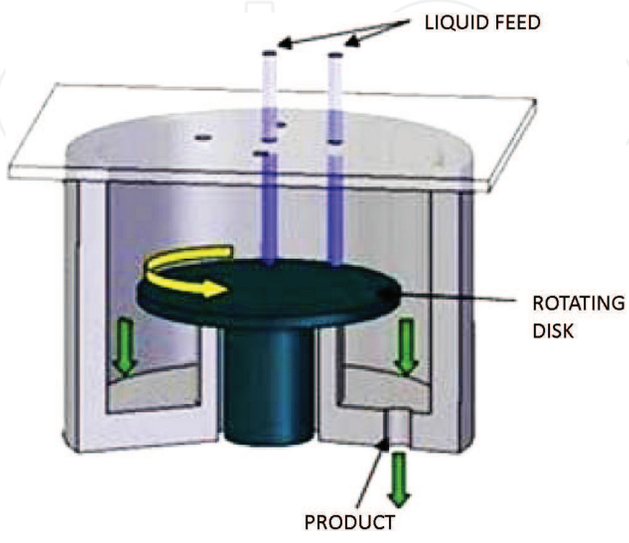

Figure 1. Scheme of the adopted SDR.

surface as a function of the distance from the disk center could be chosen between 0 and 3 cm. The constancy of the feed flow rates of each reagent solution stream was assured by the use of peristaltic pumps.

The produced suspension left the disk in continuous mode from its periphery and then suddenly came out of the cylindrical case. All the experiments were conducted at room temperature.

3. Experimental results

In the following two sections, the major results pertaining to the experimental tests conducted for the synthesis of HAP and Mg-doped HAP nanoparticles are reported. The detailed description of the adopted experimental procedures and the extensive discussions on the obtained results are reported in the cited papers.

3.1. Production process of HAP

In case of pure HAP production, three solutions were fed over the disk surface: the two reagent solutions at a distance from the disk center of 2 or 3 cm and an aqueous solution of ammonium hydroxide at the disk center. In particular, a 10% aqueous solution of NH_4OH at a flow rate of 80 ml/min was fed, whereas the two reagent aqueous streams had both a flow rate of 100 ml/min and a solute mass fraction of 5.6% of $CaCl_2$ and 3.5% of $(NH_4)_2HPO_4$, respectively. The calcium/phosphate (Ca/P) ratio of 1.67, corresponding to stoichiometric HAP, was respected. This condition is considered by many researchers very important in order to obtain nanoparticles of hydroxyapatite with high purity [17].

The reaction takes place between calcium chloride and ammonium phosphate, in the presence of ammonium hydroxide, according to the stoichiometry:

$$10CaCl_2 + 6(NH_4)_2HPO_4 + 8NH_4OH \rightarrow Ca_{10}(PO_4)_6(OH)_2 + 20(NH_4)\,Cl + 6H_2O \quad (1)$$

Ammonium hydroxide is used to attain a pH value equal to 10 and, as a consequence, high yield of the reaction to HAP [17]. Particle size distribution was measured by a dynamic light scattering instrument (DLS, PLUS 90 by Brookhaven) in the range 1–6000 nm. The samples were prepared by dispersing small amounts of the HAP powder in a 25-mL NaOH solution (0.1 M, pH 10) with 0.2 g of the surfactant Twin60 and submitting this suspension to ultrasonication for 15 min.

The experiments were focused on the evaluation of the effects of the rotational speed and of the radial distance of reagent feeding points from the disk center on the size of the HAP particles. In fact, these two parameters strongly affect the local micromixing time and as a consequence the achieved nucleation rate.

The majority of the experimental tests were carried out, feeding the reagents at 2 cm from the disk center and varying the rotational speed between 58 rad/s and 147 rad/s. Furthermore, in order to evaluate the effect of the feeding point, two runs were performed, at constancy of rotational speed of 147 rad/s, by feeding the two reagents at opposite distance of 3 cm from the center.

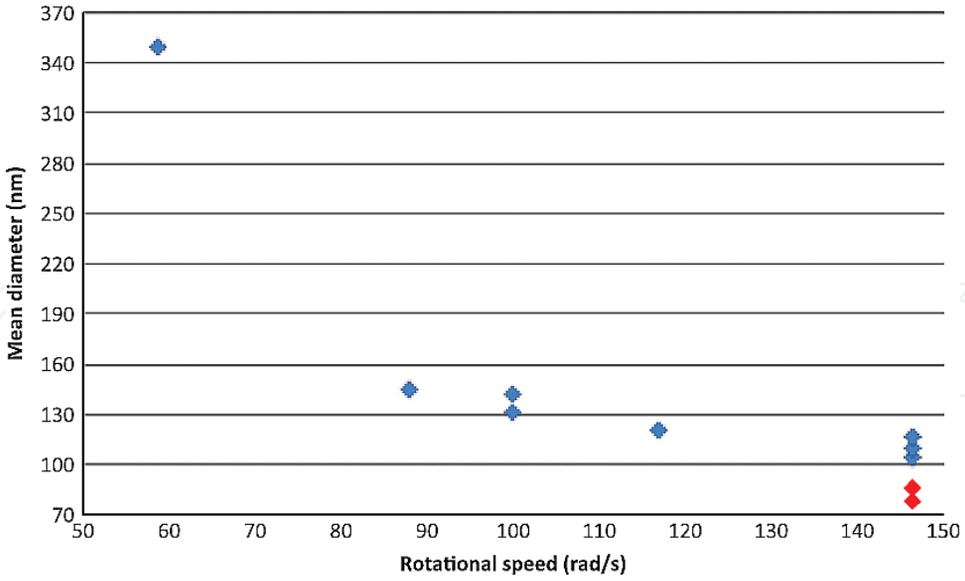

Figure 2. Average size of the produced particles, varying the rotational speed and the injection position. Blue points and red point refer to an injection point at 2 and 3 cm from the disk center, respectively.

The measured particle size as a function of rotational speed and feeding point distance is reported in **Figure 2**. As expected, the mean size of the produced particles is inversely proportional to the local energy dissipation due to the centrifugal force. In fact, this latter becomes higher when the disk rotational velocity increases and the radial position of the feed point approaches the disk edge. The minimum size, equal to 78 nm, was obtained using a rotational velocity of 147 rad/s and feeding points of reagents 3 cm from the disk center.

A typical size distribution measurement of the HAP nanoparticles is reported in **Figure 3**.

It has to be noticed that the produced nanoparticles, even in the nanometers range, are aggregations of single particles around 5 nm in size. This is, in fact, the dimension of a single crystallite estimated using the Scherrer's formula from X-ray diffractometer measurements for particles produced at the maximum rotational speed [13, 18].

The key of a rapid mixing is to produce a region of high turbulent energy dissipation, as a matter of fact that the increase of the rotational speed provides higher energy dissipation in the liquid phase over the disk surface. The specific dispersed power, [W/kg], was calculated according to the equation proposed by Moore [19]:

$$\varepsilon = \frac{1}{2 \cdot t_{res}} \left(\left(r_e^2 \cdot \omega^2 + {v_{r_e}}^2 \right) - \left(r_i^2 \cdot \omega^2 + {v_{r_i}}^2 \right) \right) \tag{2}$$

where t_{res} is the residence time of the liquid solution on the rotating disk between an external radius, r_e, where the fluid velocity is v_{re}, and an internal radius, r_i, where the fluid velocity is v_{ri}. The residence time can be calculated by the following relationship:

$$t_{res} = \frac{2 \cdot (r_e - r_i)}{v_{r_e} + v_{r_i}} \tag{3}$$

The values of the specific dispersion energy determined for a feeding point at 2 cm far from the disk center as function of the adopted values of rotational speed are reported in **Figure 4**. In this figure, the value of ε calculated for a feeding point 3 cm far from the disk center and at 147 rad/s is also reported. It is clear that increasing the disk speed and the distance of the feeding point from the center higher energy dissipation power occurs, producing better mixing conditions.

In conclusion, by increasing the local specific energy dispersion over the disk surface, micromixing at the contact point of the two reagent solutions is enhanced and HAP nanoparticles of smaller size are produced.

3.2. Production process of mg-doped HAP

It is well known that trace quantities of cations (i.e., Mg^{2+}, Zn^{2+}, Sr^{2+}) and/or anions (i.e., SiO_4^{4-}, F^-, CO_3^{2-}) in HAP play a pivotal role in its overall biological performances. Among substituting cations, magnesium is widely studied, being the fourth most abundant cation in the human body (0.44–1.23 wt%). Mg^{2+} substitution plays an essential role in the biologic environment due to its strong impact on the mineralization process, influencing both HAP crystal formation and growth [20], and increasing the HAP dissolution in human physiologic medium. In this work, the chance to produce Mg-doped nanoparticles by precipitation using

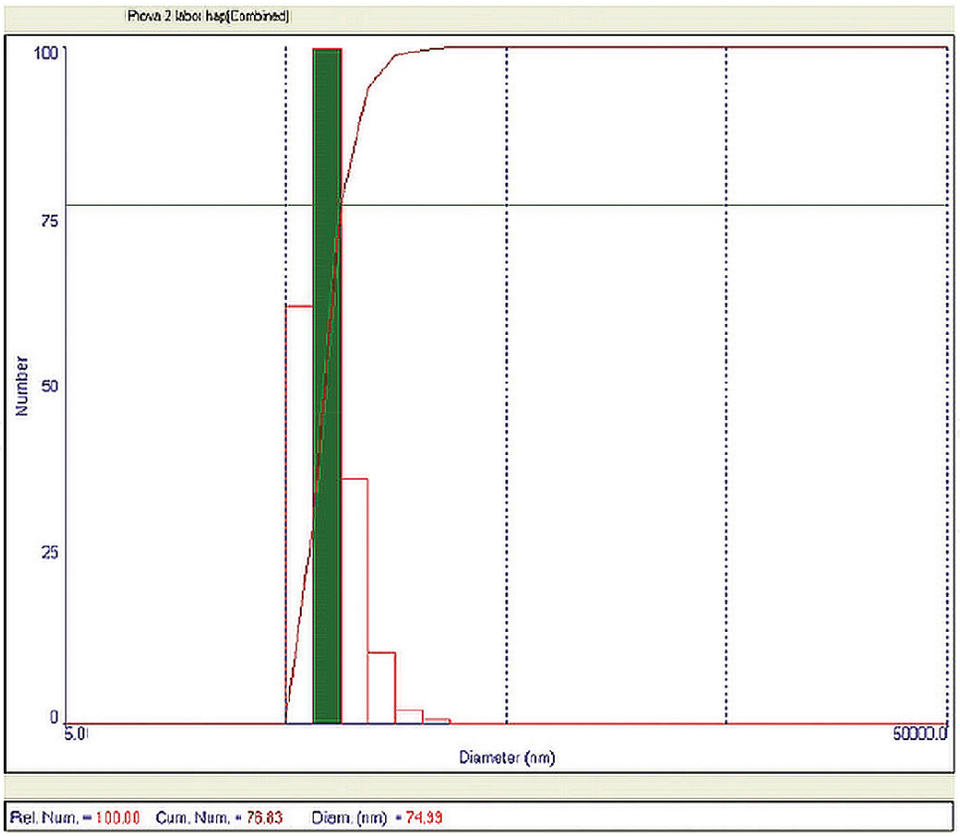

Figure 3. Size distribution measurement of HAP nanoparticles obtained with a rotational speed of 147 rad/s.

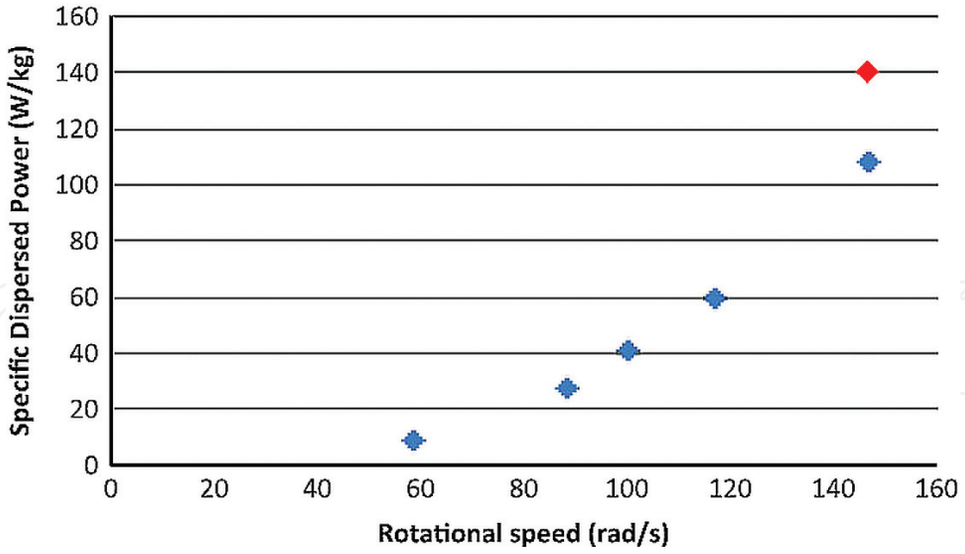

Figure 4. Specific dispersed power as a function of the rotational speed and reactant injection position. Blue points and red point refer to feed points at 2 and 3 cm from the disk center, respectively.

an SDR has been proven and the influence of the operating parameters on the nanoparticles size was investigated.

Mg-doped hydroxyapatite powders were prepared at room temperature (25°C) and air atmosphere. The precipitation reactor was performed by using the SDR 8.5 cm in diameter above described with a rotational velocity between 840 and 1500 rpm. The reaction took place among the following reagent aqueous solutions: ammonium phosphate dibasic ($(NH_4)_2HPO_4$ 0.264 M), ammonium hydroxide, (NH_4OH 2.853 M), calcium chloride ($CaCl_2$ 0.475 M) and magnesium chloride ($MgCl_2$ 0.028 M). The overall reaction was as follows:

$$(10 - x)\ CaCl_2 + xMg\ Cl_2\ 6H_2O + 6(NH_4)_2\ HPO_4 + 8NH_4OH \rightarrow Ca_{10-x}\ Mg_x(PO_4)_6(OH)_2 + 20\ NH_4Cl + 6(1 + x)\ H_2O \quad (4)$$

A value of x = 0.566 was chosen to determine a Mg^{2+}/Ca^{2+} molar ratio equal to 0.06, that is the value suggested by Landi et al. [21] to achieve the fastest bone growing rate. The NH_4OH solution was fed at the disk center, whereas the feed points of the two other reagent solutions were symmetrically located at 2 or 3 cm from the center of the disk. The details of the experimental work are reported elsewhere [22]. After each run, the obtained nanoparticles were first separated by the mother solution, then washed several times and dried for 96 h in a furnace at 80°C.

The size measurements of the produced particles were taken as above described. The X-ray diffraction (XRD) characterization of the HAP particles was performed using an XRD diffractometer (Philips PW1830 DY3558 Cu Kα, 40 kV, 30 mA). The analysis was made over a 2θ range of 2–70° at a scan rate of 0.5°C/min, with a sampling interval of 2.5 h. The crystallites average dimension was estimated from the X-ray diffractometer using the Scherrer's equation.

In addition, the B.E.T. surface area of the powder was measured by the Monosorb instrument supplied by Quantachrome. The adsorbed gas was N_2 (30%) and He (70%) at −196°C. The

morphology of the powder was examined by scanning electron microscopy (SEM, 10 Auriga 405 Carl Zeiss). Infrared spectra of Mg-HAP powder were obtained using an infrared Fourier-transform spectrometer (FTIR, VERTEX 70 model by Bruker). Finally, in order to determine both HAP stoichiometry and the Mg^{2+}/Ca^{2+} molar ratio, chemical analysis of Mg^{2+} and Ca^{2+} was done by atomic absorption spectrophotometry (AAS, Agilent Technologies 200 series AA).

In the preliminary work, the effect of the rotational speed and the reagent flow rate on the nanoparticle size was noticed; thus, accordingly, two experimental work series were carried out to investigate the influence of these two operating variables. In **Tables 1** and **2** are reported the obtained results in terms of the nanoparticles size by changing the SD rotational speed and the overall flow rate of the reagent solutions, respectively.

The rotational speed has a very strong effect on the nanoparticle size (**Table 1**), as noticed in the experimental work on pure HAP, because of the influence of the hydrodynamics on the local micromixing. By feeding the reagent solutions at 2 cm from the disk center, comparable results are obtained at rotational speed equal to or higher than 1120 rpm because similar conditions of almost complete micromixing in the liquid over the SDR surface were attained. Moreover, from the results in **Table 1**, it is clear that the feed location largely affects the size of the produced particles. For a feed location at 3 cm from the disk center, at all the rotational speed, the size of the obtained particles was less than 100 nm and smaller than one of the particles obtained for the feed location at 2 cm from the disk center. In order to interpret the obtained results, it is useful to take into account that in any case the obtained particles are agglomeration of single nanoparticles, whose size is mainly affected by the local micromixing. The larger the micromixing, due to the increase in the rotational speed (**Table 1**), the smaller the single produced particles. The effect of crystal collision on the nanoparticle size is clearly shown by the results reported in **Table 2**, performed at constancy of rotational speed. By increasing the overall reagent solution flow rate, the residence time of the particle slurry suspension decreases and the probability of collisions as well. As a consequence, the smallest particle size is achieved at the maximum flow rate of 4 ml/s. In particular, by increasing eight times the overall feed flow rate from 0.5 up to 4 ml/s, the average size of the agglomerated particles decreases from 71 down to 52 nm.

The image of the nanoparticles obtained at the best operating conditions, that is, at 1400 rpm, location point 3 cm from the center and overall reagent solution flow rate of 4 ml/s, is reported in **Figure 5**.

SD rotational speed rate (rpm)	**SD rotational speed rate (rpm)**	
	Feed location at 2 cm	**Feed location at 3 cm**
840	392.8	97.0
980	305.1	71.7
1120	80.2	64.3
1260	75.2	56.9
1400	72.3	51.3

Table 1. Average particle size at different SD rotational speed (overall flow rate of the reagent solutions equal to 3 ml/s).

The average size and the standard deviations along the two geometrical axes are, respectively, 169 and 36 nm, along the major axis and 33 and 7 nm along the minor axis, and thus, the nanoparticles exhibit a length/width ratio around 5. The XRD pattern of the synthesized Mg-doped powder reported in **Figure 6** confirmed a nanocrystalline single-phase HAP and allowed

Overall liquid feed flow rate (ml/s)	**Particle size (nm)**	
	Average size	**Standard deviation**
0.5	70.7	5.4
1.0	58.8	7.4
2.0	51.9	6.8
3.0	51.3	7.8
4.0	51.3	7.8

Table 2. Nanoparticle size of mg-doped HAP at different values of the overall feed flow rates (feed location at 3 cm from the center and rotational speed equal to 1400 rpm).

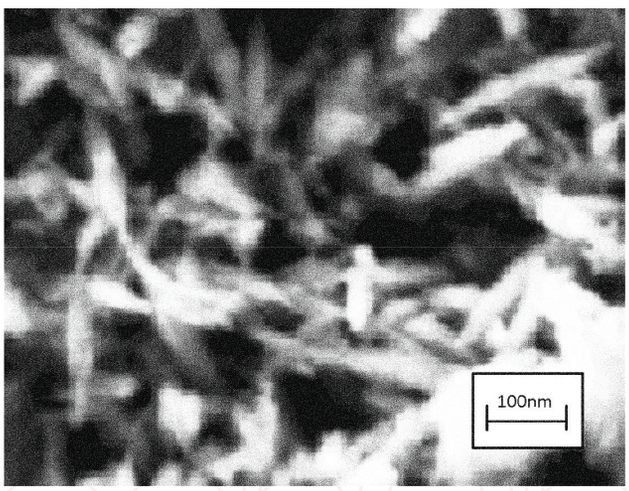

Figure 5. SEM image of the mg-doped HAP nanoparticles obtained at the best operating conditions.

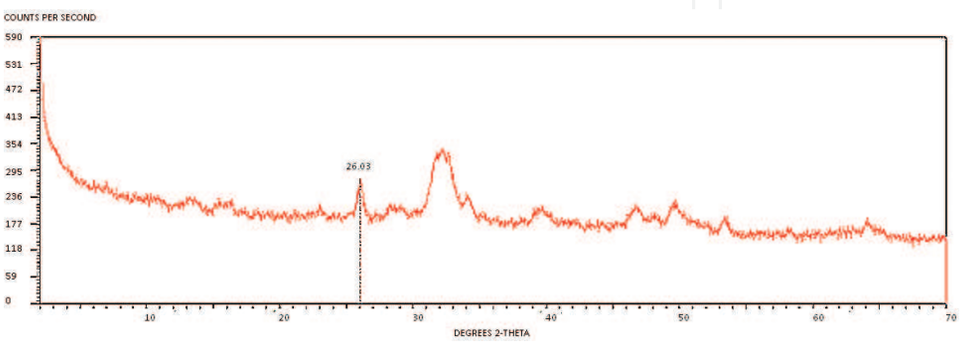

Figure 6. XRD pattern of the produced mg-HAP powder.

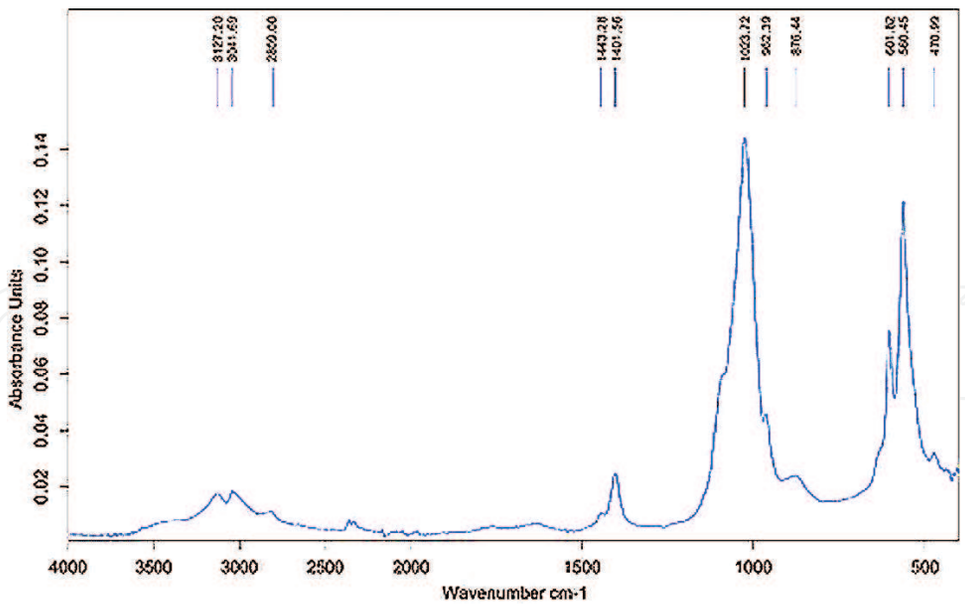

Figure 7. FT-IR spectra of the produced mg-HAP sample.

to estimate crystallite dimension of 5 nm by applying the Scherrer's formula. The estimated size of the crystallites is consistent with the hypothesis of agglomeration for the produced particles.

The B.E.T. results gave a specific area of 132.6 m^2/g, which is higher than the values reported by Landi [21], in the range 90–125 m^2/g. The FT-IR spectra reported in **Figure 7** show the typical phosphate bands of hydroxyapatite compounds located at 980–1100 cm^{-1} (asymmetric stretching) and at 560–600 cm^{-1} (asymmetric bending).

Finally, from the Mg-HAP analysis by atomic adsorption spectrophotometry a molar ratio Mg^{2+}/Ca^{2+} equal to 0.06 resulted, in according with the target fixed in this work.

4. CFD modeling of the SDR performance in HAP synthesis

The progressive progress in computational fluid dynamics (CFD) techniques and in the available computing power encourages the application of this modeling approach across multiple engineering fields and, in particular, in the area of chemical reaction engineering. However, in the case of spinning disk reactors applied to the synthesis of nanoparticles, a few of CFD studies are present in literature, in spite of the expected benefits for the physical interpretation of the occurring physical–chemical phenomena. In this section, a careful attempt has been made to model the hydrodynamics of the three-phase system over the disk surface and to interpret the obtained experimental results with reference to the HAP nanoparticles production.

SDR performances are strongly affected by the adopted operating conditions. Consequently, a fine description of thin-film hydrodynamics appears as essential in studying and optimizing the operating conditions of an SDR.

The use of an SDR should promote the mixing among the reagents, which leads to very low micromixing time, less than 1 ms, to maximize the reagent concentrations and one of the

products. In case of no adequate mixing, in fact, the two reagent solution streams may give rise to a wide segregate area where one of the reagents predominates. Once this segregation is established, the reaction occurs mainly outside the selected pH value, producing the formation of larger particles which tend to agglomerate away from their feed point because of the high residual product concentration.

To avoid this unfavorable situation, the optimal condition should be set, promoting a rapid mixing of the reagent streams, maximizing the reaction rate between the reagents, where high nucleation rate occurs, and minimizing the residual supersaturation available for the growth of the formed particle.

These conditions are all favored by a high velocity field in the overall film thickness developed on the disk. Some simplified descriptions of the film hydrodynamics were proposed in literature, starting from the simplified Nusselt model, the Pigford, Lepehin and Riabchuk models, just to mention a few. As matter of fact, Burns et al. [9] reported that the Nusselt model returns a rough description of the film thickness at high Ekman numbers, with an average overprediction around 10%. Based on the experimental results reported in this Burns' work, Bhatelia et al. [10] implemented and validated a CFD model where no specific liquid film turbulence was addressed, producing results not enough accurate to grasp the true film hydraulics.

The approach here proposed to simulate the behavior of the reaction precipitation system over the adopted SDR moves from a CFD hydrodynamic model developed by de Caprariis et al. [11]. In this study, the CFD model is extended to the prediction of the average size of the produced HAP nanoparticles. The hydroxyapatite production was studied with the aim to predict the SDR performances at various operating conditions. A nanoparticle diameter estimation to be compared with the available experimental data was derived by the implementation of a population balance equation (PBE).

As previously described, the production of nanoparticles of hydroxyapatite by chemical precipitation reaction took place in an SDR operating in continuous mode and consisting of an inner rotating disk 8.5 cm in diameter. Three reagent solutions were injected onto the disk at three selected feed points: the ammonium hydroxide at the distance of 1 mm from the disk and the other two reagents at 2 cm from the disk center, in opposite positions.

The first step of the simulation procedure consisted of the generation of a stable, stationary and continuous liquid film onto the disk surface. This initial condition was addressed by feeding only the NaOH water solution (10%wt) at the rate of 80 ml/min. Once a stationary liquid phase was established, the two reagents $CaCl_2$ and $(NH_4)_2HPO_4$ were continuously fed in the form of water solution (5.6 and 3.5%wt, respectively), both at the same flow rate of 100 ml/min, at a position of 2 cm from the disk center. A calcium/phosphate (Ca/P) stoichiometric ratio of 1.67 was assumed. The rotational velocity was fixed at 146.5 rad/s. The reaction takes place between calcium chloride and ammonium phosphate, in the presence of ammonium hydroxide, according to the stoichiometry described by Eq. (1).

On the basis of the disk geometry, a computational grid necessary to resolve the CFD model was built in the Gambit environment. The computational domain has considered only the zone of the disk from a radius of 2 cm ahead, that is where the liquid height is approximately constant and the reaction takes place. In fact, according to the liquid profiles reported in

Figure 8, in the examined domain the film thickness is quite constant and it is the only one where the reaction occurs, since the reagents are injected 2 cm away from center of the disk. Therefore, the adopted grid for the simulation work consists of a cylinder 8.5 cm in diameter and 70 μm in height, composed by 260,000 cells. The mesh is structured and made of hexahedral cells, so that the flux is orthogonal to the faces of each cell in the radial direction, limiting the numerical diffusion errors especially in the presence of convective fluxes.

The numerical simulations were performed in the ANSYS Fluent v.14.5 environment, a commercial CFD package based on finite volume resolution method. The reaction was modeled according to the Eulerian multiphase model. This model was chosen because the length of the interface between the forming crystals and the liquid medium is by far shorter than the characteristic length of the computational domain. In the framework of this model, the physical system was simulated by a continuous liquid phase containing all the reacting species and a solid phase consisting of the nucleating hydroxyapatite nanoparticles formed by the reaction. The Eulerian model solves a set of n continuity and momentum equations for each phase, coupled through the interphase and pressure exchange coefficients. The turbulence was modeled according to *k*-epsilon model.

The precipitation reaction was described according to the finite rate model implemented with literature kinetic data [23]. The set of equations consists of the balances of momentum, mass, energy and solid particle population. The population balance equation (PBE) aiming to predict the size distribution of the particles is written in terms of density function $n(V,t)$ as follows:

$$\frac{\partial}{\partial t}[n(V,t)] + \nabla\left[\vec{u}\; n(V,t)\right] + G = A_B + A_D + B_B + B_D \tag{5}$$

where $\dot{n_V}$ is the nucleation rate (#/m^{3}s). The PBE can be solved once the boundary and initial conditions are set:

- BC: $n(V=0,t) = \dot{n_0}$
- IC: $n(V,t=0) = n_V$

In the PBE, G is the growth term, A_B and A_D are the birth and death rate due to aggregation terms, respectively, and B_B and B_D are the birth and death rate due to breakage terms, respectively. In the considered process, however, all the terms, apart from the nucleation

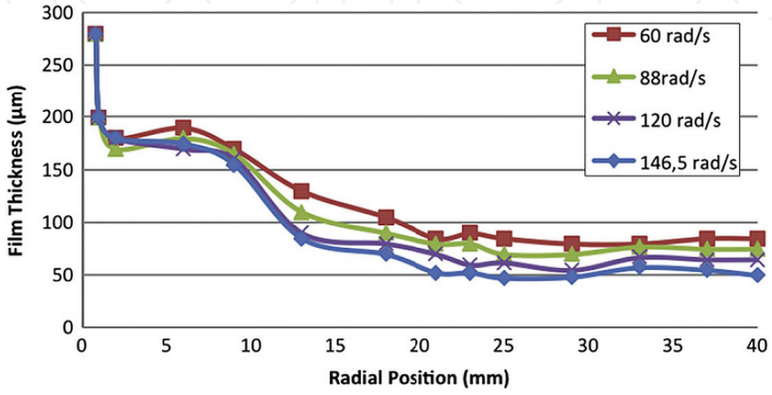

Figure 8. Film thickness profile [10].

contribution, have been ignored due the particular characteristics of the reaction. In fact, when the precipitation reaction takes place at complete micromixing conditions, it can be considered that most of the supersaturation ratio, that is, the driving force, is consumed by the nucleation, leaving only a reduced driving force for the remaining phenomena, that is, solid growth and aggregation. A constant nucleation rate $n\dot{i}_V$ = 10^{11} #/m^3s, equal to an average value derived from the literature data for this class of reactions, was assumed.

The PBE can be solved according to different approaches, and in this chapter, the Quadrature Methods of Moments (QMOM) was adopted [24]. This model allows the calculations of the moments describing the population balance through a relatively reduced set of equations, furthermore limiting the computational errors. The main advantages of this approach are to involve few variables (from six to eight different moments) and to allow the dynamic calculation of the size bins, obtained however at a quite high computational cost. Further details about the model choice and its setting are reported by Dugo [25]. The main results of the CFD simulation are briefly shown and discussed below.

The tangential velocity profiles of the liquid phase at the disk surface and at the liquid film maximum height resulted by the CFD simulation are reported in **Figure 9**. The liquid velocity continuously increases from the center to the periphery of the disk, as expected.

The contours of the concentrations of the two reagent streams computed at the middle of the film (35 μm) are reported in **Figure 10**. These contours show that the maximum concentration of each reagent at the feeding point progressively lows down along the disk, due to the reaction occurrence. It has to be noticed that from the quantitative point of view the complete mixing gives rise along the disk to an average stoichiometric ratio between the two reagents of approximately 1.67.

The precipitation reaction is nearly instantaneous and starts as soon as the reagent streams get in contact. Hence, the maximum reaction rate is located at the contact points, as clearly shown in **Figure 11**.

The HAP mass fraction contour showed in left side of **Figure 11** confirms that the HAP production starting point occurs at the feed point of the two reagents, where the calculated reaction rate shows the highest values (right side of **Figure 11**). From these points, ahead the

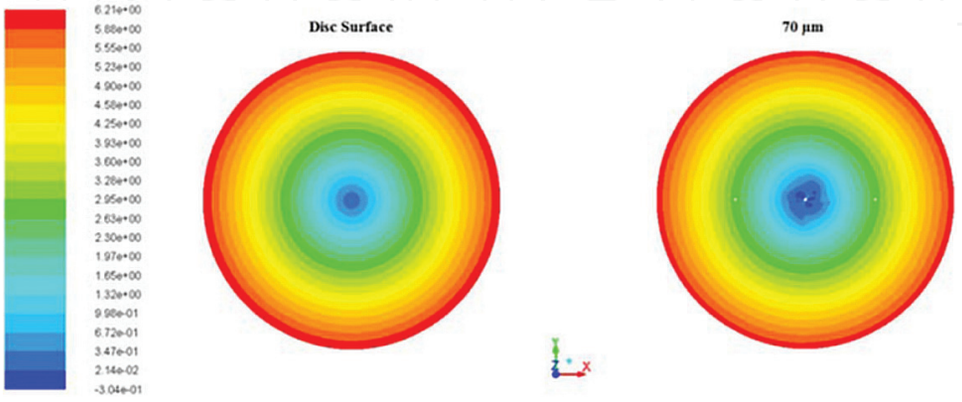

Figure 9. Tangential velocity profiles of the liquid phase at the disk surface and at the maximum film height (70 μm).

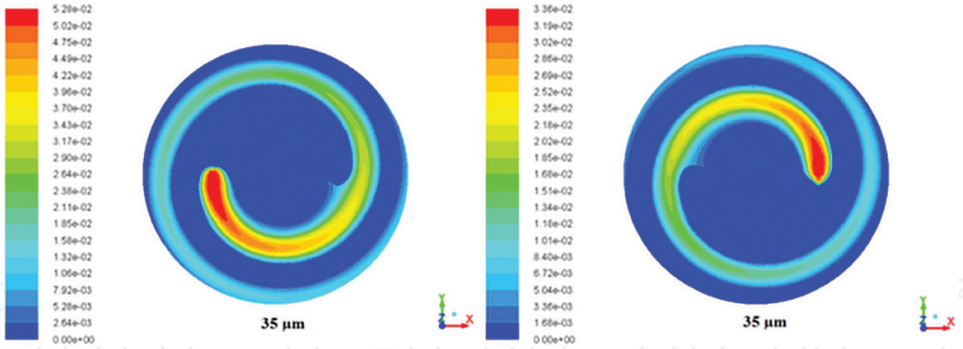

Figure 10. Reagent concentration contours at a film height of 35 µm: $CaCl_2$ left, $(NH_4)_2HPO_4$ right.

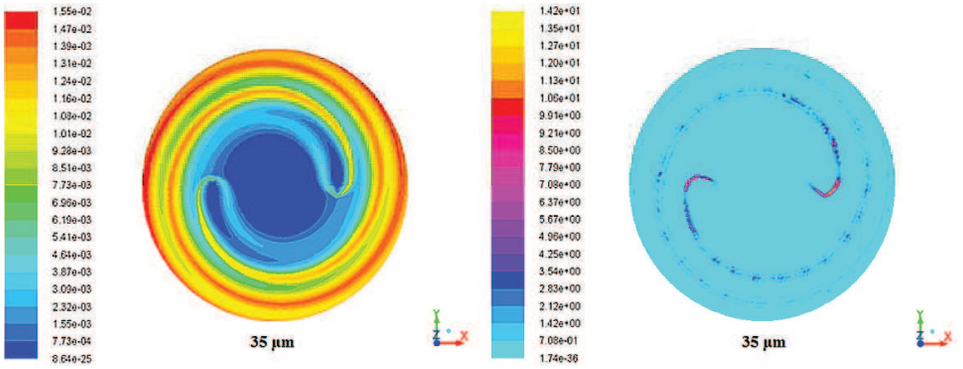

Figure 11. Hydroxyapatite concentration contour in the liquid phase at a film height of 35 µm, left. Reaction rate contour, right.

HAP concentration increases for the advances of the reaction along the disk until a maximum concentration at the disk edge.

On the basis of the calculated mass produced by the reaction, the HAP crystallite dimension was predicted by means of the PBE as here after detailed.

The results of concern of the PBE solution are the moments of different orders that are directly related to the particle diameters. In particular, the moments of order from 0 to 3 are linked to the representative diameters, d_{10} and d_{32}, by Eqs. (6) and (7), respectively:

$$d_{10} = \frac{m_1}{m_0} \tag{6}$$

$$d_{32} = \frac{m_3}{m_2} \tag{7}$$

Because the estimation of the d_{32} diameter is based on the m_2 and m_3 moments, linked to the surface and volume shape factors, respectively, the corresponding figure can be considered more accurate in inferring the true particle size.

The values of the moments calculated at the disk edge are shown in **Table 3**, allowing the estimation of the formed nanoparticle size in the range d_{10} = 2.19 nm and d_{32} = 4.8 nm. These results should be considered as referring to the dimension of the crystallite, that is, the crystals

Moments	
m_0	4.12×10^{7}
m_1	9.04×10^{-2}
m_2	1.63×10^{-11}
m_3	7.82×10^{-20}

Table 3. Values of the moments obtained from the simulations.

born due to the nucleation phenomenon, since no crystal growth and agglomeration phenomena were taken into account in the simulations.

The dimension of the crystallite of hydroxyapatite was measured in previous works [13, 22] with X-ray diffraction technique, calculating the value of the diameter by the Scherrer's formula. The images of the HPA crystals reported in Section 3 and considered as agglomerated crystals are consistent, and the estimated crystallite diameter is about 5 nm. The d_{32} value obtained from the CFD simulation proves, thus, the reliability of the developed model.

5. Conclusions

The biocompatible characteristics of hydroxyapatite are emphasized when its mass has a very high specific surface, as in case of nanoparticles. In this chapter, it has shown that the HAP production process can be effectively performed by chemical precipitation by using a spinning disk reactor. By operating at a disk rotational speed of 1500 rpm, pure HAP nanoparticles around 70 nm are obtained. When the reaction is operated in the presence of $MgCl_2$, Mg-doped HAP nanoparticles are obtained down to 51 nm in size. In this case, the adopted analytical techniques ascertained both the nature of HAP and a molar ratio Mg^{2+}/Ca^{2+} equal to 0.06, needed to achieve the fastest bone growing rate. The results in terms of the obtained nanoparticle sizes are worthwhile because they refer to a production process which can be carried out in continuous mode, whereas most of the results in literature concern preparation in batch mode. In this chapter, the effects of the disk rotating speed and the feed location of the reagent solutions on the produced particle size were clearly shown and discussed. Then, a CFD model was developed in order to describe the hydrodynamics and the reaction-precipitation process in the film thickness formed over the SDR surface. The interest in developing such a tool relies in the possibility to predict the outcome of reagent mixing and chemical reaction processes into the system domain, a prerequisite to estimate the particle size distribution of the product obtained by chemical precipitation.

The results show that the SDR is an effective device in performing this class of reactions where the mixing of the reagents is of fundamental importance. Hydroxyapatite, indeed, is produced in the liquid phase instantaneously as soon as the reagents enter in contact. The population balance equation added to the hydrodynamic model allows an estimation of the particle diameters. Because only the nucleation was taken into account in the PBE equation, the prediction concerned only the size of the HAP crystallite, which results of 4.3 nm. This value is in a good agreement with literature experimental data.

Author details

Benedetta de Caprariis, Angelo Chianese, Marco Stoller and Nicola Verdone*

*Address all correspondence to: nicola.verdone@uniroma1.it

Department of Chemical, Material, Environmental Engineering, Sapienza University of Rome, Rome, Italy

References

[1] Paz A, Guadarrama D, López M, González JE, Brizuela N, Aragón J. A comparative study of hydroxyapatite nanoparticles synthesized by different routes. Quimica Nova. 2012;**35**:1724-1727

[2] Hung LH, Lee AP. Microfluidic devices for the synthesis of nanoparticles and biomaterials. Journal of Medical and Biological Engineering. 2007;**27**:1-6

[3] Cafiero LM, Baffi G, Chianese A, Jachuck RJJ. Process intensification: Precipitation of barium sulphate using a spinning disc reactor (SDR). In: Proceedings of 14th European Symposium on Ind. Crystallization; 12–16-09-1999; Cambridge

[4] Baffi G, Cafiero ML, Chianese A, Jachuck RJJ. Process intensification: Precipitation of barium sulphate using a spinning disc reactor (SDR). Industrial and Engineering Chemistry Research. 2002;**41**:5240-5246

[5] Trippa G, Hetherington P, Jachuck R. Process intensification: Precipitation of calcium carbonate from the carbonation reaction of lime water using a spinning disc reactor. In: Proceedings of 15th International Symposium on Industrial Crystallization; 15-18-09-2002; Sorrento, Italy

[6] Raston CL, Anantachoke N, Makha M, Reutrakul V, Smith NC, Saunders M. Fine tuning the production of nanosized b-carotene particles using spinning disc processing. Journal of the American Chemical Society. 2006;**128**:13847-13853

[7] Loh JW, Schneider J, Carter M, Saunders M, Lim L. Spinning disc processing technology: Potential for large-scale manufacture of chitosan nanoparticles. Journal of Pharmaceutical Sciences. 2010;**99**:4326-4336

[8] Dabir H, Davarpanah M, Ahmadpour A. Effects of different operating parameters on the particle size of silver chloride nanoparticles prepared in a spinning disc reactor. Applied Physics A. 2015;**120**:105-113

[9] Burns JR, Ramshav C, Jachuck RJ. Measurement of liquid film thickness and the determination of spin-up radius on a rotating disc using an electrical resistance technique. Chemical Engineering Science. 2015;**58**:2245-2253

[10] Bhatelia TJ, Utikar RP, Pareek VK, Tade MO. Characterizing liquid film thickness in spinning disc reactors. Proceedings of the 7th International Conference on CFD in the Minerals and Process Industries; 9–11-12-2009; Melbourne, Australia

[11] de Caprariis B, Di Rita M, Stoller M, Verdone N, Chianese A. Reaction-precipitation by a spinning disc reactor: Influence of hydrodynamics on nanoparticles production. Chemical Engineering Science. 2012;**76**:73-80

[12] Plasari E, Muhr H, Rousseaux JM, Vial C. CFD simulation of precipitation in the sliding-surface mixing device. Chemical Engineering Science. 2001;**56**:1677-1685

[13] de Caprariis B, Stoller M, Chianese A, Verdone N. CFD model of a spinning disc reactor for nanoparticle production. Chemical Engineering Transactions. 2015;**43**:757-761

[14] Hounslow MJ, Mumtaz HS. Aggregation during precipitation from solution: An experimental investigation using a Poiseuille flow. Chemical Engineering Science. 2000;**55**:5671-5681

[15] Parisi M, Stoller M, Chianese A. Production of nanoparticles of hydroxyapatite by using a spinning disc reactor. Chemical Engineering Transactions. 2011;**24**:211-217

[16] Stoller M, Miranda L, Chianese A. Optimal feed location in a spinning disc reactor for the production of TiO_2 nanoparticles. Chemical Engineering Transactions. 2009;**17**:993-999

[17] Martins MA, Santos C, Almeida MM, Costa MEV. Hydroxyapatite micro- and nanoparticles: Nucleation and growth mechanisms in the presence of citrate species. Journal of Colloid and Interface Science. 2008;**318**:210-216

[18] Pang YX, Bao X. Influence of temperature, ripening time and calcination on the morphology and crystallinity of hydroxyapatite nanoparticles. Journal of the European Ceramic Society. 2003;**23**:1697-1704

[19] Moore SR. Mass Transfer to Thin Liquid on Rotating Surfaces with and without Chemical Reaction [Thesis]. University of Newcastle upon Tyne; 1986

[20] Pina S, Olhero S, Gheduzzi S, Miles A, Ferreira J. Influence of setting liquid composition and liquid-to-powder ratio on properties of a mg-substituted calcium phosphate cement. Acta Biomaterialia. 2009;**5**:1233-1240

[21] Landi E, Logroscino G, Proietti L, Tampieri A, Sandri M, Sipro S. Biomimetic mg-substituted hydroxyapatite: From synthesis to in vivo behavior. Journal of Materials Science. Materials in Medicine. 2008;**19**:239-247

[22] D'Intino AF, de Caprariis B, Santarelli ML, Verdone N, Chianese A. Best operating conditions to produce hydroxyapatite nanoparticles by means of a spinning disc reactor. Frontiers of Chemical Science and Engineering. 2014;**8**:156-160

[23] Liu C, Huang Y, Shen W, Cui J. Kinetics of hydroxyapatite precipitation at pH 10 to 11. Biomaterials. 2001;**22**:301-306

[24] Marchisio DL, Virgil RD, Fox RO. Quadrature method of moments for aggregation-breakage processes. Journal of Colloid and Interface Science. 2003;**258**:322-334

[25] Dugo F. Modellizzazione fluidodinamica di un reattore a disco rotante per la produzione di nanoparticelle di idrossiapatite [Master Thesis]. Library of the Chemical Engineering Department. Sapienza University of Rome; 2014